I&EC research
Industrial & Engineering Chemistry Research

Article

Cite This: Ind. Eng. Chem. Res. 2019, 58, 20722−20733

pubs.acs.org/IECR

Design of Robust PI Controller with Decoupler for a Fluid Catalytic Cracking Unit

Prabhu Teja Y[†,‡] and C. Sankar Rao*[,†]

[†]National Institute of Technology Karnataka, Surathkal 575025, India

[‡]Department of Chemical Engineering, National Institute of Technology Karnataka, Surathkal 575025, India

ABSTRACT: In this work, a decoupling control system is designed for the riser section of the fluid catalytic cracking unit (FCCU). The decentralized control system is implemented on FCCU to estimate the magnitude of the interactions using relative gain array (RGA). Interactions among the loops are minimized by applying the decoupling control strategy to decentralized FCCU. Relative normalized gain array and dynamic relative gain array (dRGA) are computed for the closed-loop FCCU and used to design the decouplers for the process. The advantages of the decoupling control strategy are a simple design and it does not need extensive calculations. This method gives a dynamic decoupler in the form of lead/lag modules with time delays. PI controllers can be designed efficiently for controlling the riser temperature, mass fractions of gasoline, and LPG. The decentralized controller and the decoupling control system performances are studied on the basis of the closed-loop performance of control variables, and it is found that the decoupler performs better.

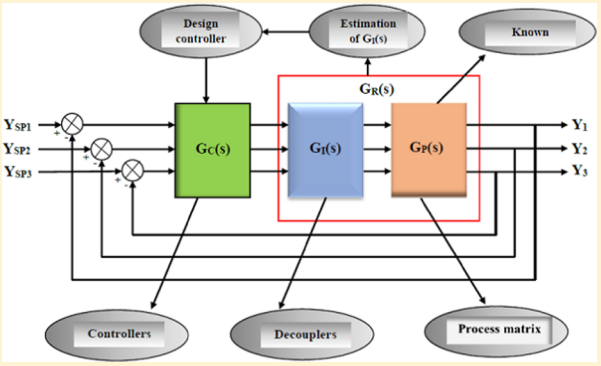

INTRODUCTION

Petroleum refineries start with the atmospheric distillation unit followed by vacuum distillation unit (VDU). The bottom product of VDU contains a mixture of high-molecular-weight components. A fluidized catalytic cracking unit (FCCU) is placed after the VDU to produce valuable products by cracking the higher-molecular-weight components mixture to lower-molecular-weight components. FCCU is one of the essential unit processes in refineries due to its high conversion of heavier compounds to lighter compounds. The FCCU consists of three main units, the riser, the regenerator, and the fractionator, as shown in Figure 1. The riser reactor is a standpipe in which cracking reaction takes place. Spent catalyst from the riser reactor is sent to the regenerator reactor for coke removal and to reuse for the cracking reaction. A combustion reaction takes place in the regenerator reactor. The vapors generated in the riser due to cracking reaction are sent to a fractionator to separate the gasoline and LPG from the mixture of lighter compounds. The process of FCCU is as follows, feed to the riser is collected from the bottom product of VDU, which is known as heavy vacuum gas oil. The feed will be preheated until it converts to vapor. An endothermic reaction takes places in the riser reactor. To reach the cracking reaction temperature of the feed, it will get in contact with the regenerated catalyst from the regenerator unit. Deposition of coke takes place in riser reactor during the cracking reaction. Spent catalyst can be regenerated by burning off coke on the catalyst with a continuous supply of air.

The FCCU is quite complex from both the process modeling and control points of view.[1,2] A four-lump parameter

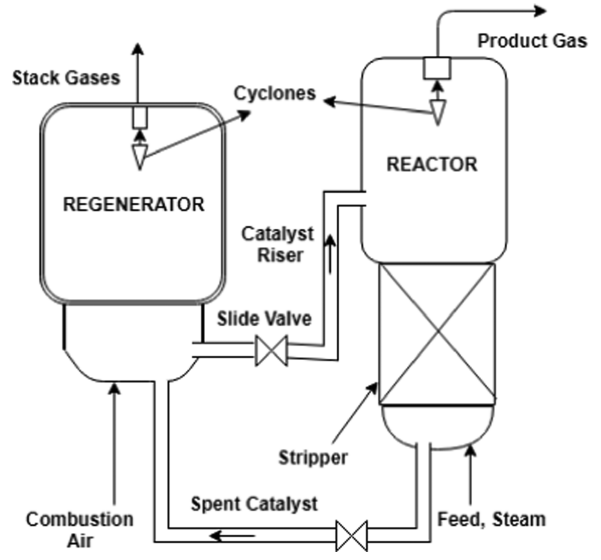

Figure 1. Schematic representation of FCCU.

is used to model the riser, regenerator, and fractionator.[3] The effectiveness of the modeling is enhanced by incorporating the effects of the volumetric expansion of feed and product gas from the riser reactor and turbulence. There are many factors

Received: August 28, 2019
Revised: October 23, 2019
Accepted: October 23, 2019
Published: October 24, 2019

DOI: 10.1021/acs.iecr.9b04770
Ind. Eng. Chem. Res. 2019, 58, 20722−20733

such as coke deposition rate,[4] the hydrodynamics of the systems,[5] and the concentrations of CO and CO_2 in the regenerator[6] that affect the performance of the model that should be considered during the system modeling. While modeling the FCCU riser reactor is considered as a plug flow reactor (PFR), regenerator is divided into two phases, one of which is the bubble phase and the other is the emulsion phase.[7] The bubble phase is modeled as the continuous stirred tank reactor, and the emulsion phase as plug flow reactor (PFR).[8,9] Dynamic response of the process is necessary to design a controller for the process. Controllers which are designed based on nonlinearity are better than the linear system.

Continuous process industries are difficult to control, one of the reasons being multivariable system. The best industrial examples of multiple input multiple output (MIMO) are distillation columns and FCCU.[10] The MIMO processes are troublesome due to their high process interactions. Designing a controller for the highly interacting system is difficult. Highly interactive systems mean that if there is a disturbance in one manipulated variable, all control variables in the system can be affected. Due to its multiloop condition, it is difficult to find the best pairing of manipulated variables and control variables. In such situation, the decentralized method is useful.[11] Multiloops are broken into n single loops in the decentralized method. Among the n single-loop controls, manipulated variables and control variables are designed for the best pairing. The relative gain array (RGA) method can be used to determine the best pairing.

FCCU is one of the best examples for a system with multiloops and high interactions. Such systems modeling leads to multivariable systems. Two types of control systems are usually available to control such systems. The first is a decentralized control system that uses single-loop controllers. The second is a centralized controller, where the control matrix is not a diagonal matrix. The decentralized controller scheme is favored over the centralized controller mainly because the control system has only n controllers for n output variables, and the operators can easily understand the control loops. The use of a decentralized and RGA approach allows controllers to be designed, but the system can sometimes be unstable due to the interactions between the loops. Decouplers should be included to eliminate interactions. Decouplers are used to remove the effect of a change in control variables due to change in a manipulated variable.[12] Dynamic decouplers, which are used for continuous systems, are designed by using dynamic relative gain matrix (dRGA) and relative normalized gain array (RNGA). Decouplers for higher-order systems and systems with high interactions are difficult to design.

Here, the relative gain array (RGA) method is used to quantify the interactions between multiloops. The temperature of the riser (T_{ris}), mass fraction of gasoline (Y_{ga}), and mass fraction of lpg (Y_{lpg}) are considered as control variables, whereas regenerated feed rate, feed temperature, and temperature of the regenerated catalyst are considered as manipulated variables. T_{ris} plays a crucial role in the conversion of gas oil. Y_{ga} and Y_{lpg} are considered as control variables because of their importance in the economy of plant. High interactions in FCCU may affect the performance of the controller. It is advised to minimize the interactions for better controller performance. For minimizing the interactions in FCCU, decouplers can be implemented. It is necessary to design the decentralized controller and decouplers for FCCU. To date, no research has been reported on the application of decentralized decoupler on FCCU. No one has reported the magnitude of the interactions in FCCU. In this work, an attempt is made to design a PI decentralized and decouplers for the FCCU.

Many research studies have been carried out over the years on the control of the FCC. The tuning methods for the controller are improved considerably over the time. Nevertheless, no research has been reported on the implementation of the decentralized controller on the FCC unit. Multivariable processes are troublesome to handle with a single PI controller. This work deals with the design of a decentralized controller and decoupler for the control of the riser temperature in the FCCU. An easy and efficient way of handling multivariable processes is by implementing a decentralized controller with decoupler by considering the interactions among measured and manipulated variables.

METHODOLOGY

In continuous process industries such as petroleum refineries, multiple outputs must be controlled simultaneously by multiple inputs. A multiple-input multiple-output (MIMO) system can be controlled by decentralizing the MIMO process into l^2 single-input single-output (SISO) processes, where l is the number of outputs. This set of SISO processes is given as follows

$$\begin{pmatrix} y_1 \\ y_2 \\ y_3 \end{pmatrix} = \begin{pmatrix} g_{11} & g_{12} & g_{13} \\ g_{21} & g_{22} & g_{23} \\ g_{31} & g_{32} & g_{33} \end{pmatrix} \begin{pmatrix} u_1 \\ u_2 \\ u_3 \end{pmatrix} \quad (1)$$

$$Y = G_p U \quad (2)$$

where Y is the (3×1) vector of the output variable, G_p is the (3×3) process transfer function matrix, and U is the (3×1) vector of the input variables.

Decentralized Controller. This section presents a method for designing a decentralized control system for three inputs and three outputs. A schematic representation of decentralized controller for a (3×3) system is shown in Figure 2. The first

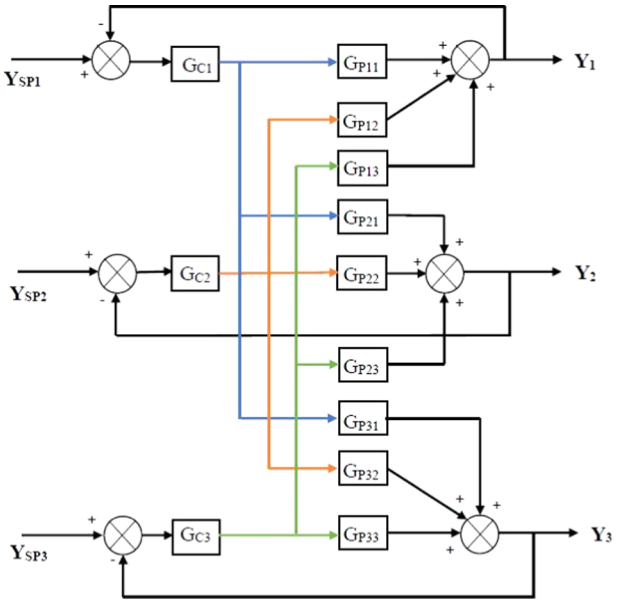

Figure 2. Decentralized system for three inputs and three outputs.

DOI: 10.1021/acs.iecr.9b04770
Ind. Eng. Chem. Res. 2019, 58, 20722−20733

step in the development of the decentralized controller is to convert all higher-order transfer functions to first-order plus time (FOPTD).[13] The higher-order transfer function models are approximated to FOPTD using the process reaction curve method given by Sundaresan and Krishnaswami. The decentralized controller matrix can be given as

$$G_C = \begin{pmatrix} G_{C1} & 0 & 0 \\ 0 & G_{C2} & 0 \\ 0 & 0 & G_{C3} \end{pmatrix} \tag{3}$$

The decentralized PI controllers are assumed as

$$G_{Cj} = K_{Cj}\left(1 + \frac{1}{\tau_{Ij}s}\right) \tag{4}$$

where K_{Cj} and τ_{Ij} are the controller gain and the integral time constant for jth controller, respectively (here, j = 1, 2, and 3). G_{C1}, G_{C2}, and G_{C3} are designed based on the process parameters g_{11}, g_{22}, and g_{33}, respectively.

Identification of the FOPTD Model. In this work, a process reaction curve method is used to identify the FOPTD.[13,14] To obtain model parameters of FOPTD, Sundaresan and Krishnaswami developed an open-loop identification method based on the transient step response of the process. In this method, times t_1 and t_2 are obtained from the transient step response curve when the fractional responses are y_1 = $0.353\Delta y_\infty$ and y_2 = $0.853\Delta y_\infty$, respectively, as shown in Figure 3. The general form of the FOPTD model is given as

$$G_p(S) = \frac{K_P}{\tau s + 1}e^{-\theta s} \tag{5}$$

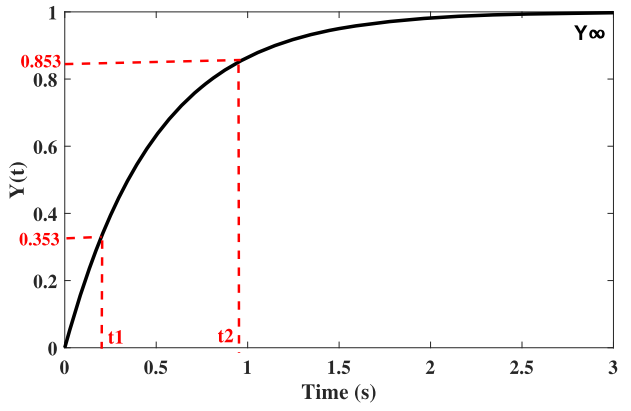

Figure 3. Process reaction curve for step input in the process.

The model parameters of FOPTD, such as time constant (τ), process gain (K_P), and time delay (θ), can be estimated as follows[13]

$$K_P = \frac{\Delta Y_\infty}{\Delta U_\infty} \tag{6}$$

$$\tau = 0.67(t_2 - t_1) \tag{7}$$

$$\theta = 1.3t_1 - 0.29t_2 \tag{8}$$

Selection of Best Pairing. [15,16] The relative gain array (RGA) is used to determine the best pairing between the control and manipulated variables. The RGA matrix can be calculated by the following equation

$$\Lambda = \mathrm{RGA} = K \otimes (K^{-1})^{\mathrm{T}} = \begin{pmatrix} \lambda_{11} & \lambda_{12} & \lambda_{13} \\ \lambda_{21} & \lambda_{22} & \lambda_{23} \\ \lambda_{31} & \lambda_{32} & \lambda_{33} \end{pmatrix} \tag{9}$$

where λ_{ij} are the elements of relative gain array, K is the gain matrix, and $\otimes$ is the Hadamard product. The gain matrix can be estimated from the process matrix (G_p) by substituting s = 0.

$$K = \begin{pmatrix} k_{11} & k_{12} & k_{13} \\ k_{21} & k_{22} & k_{23} \\ k_{31} & k_{32} & k_{33} \end{pmatrix} \tag{10}$$

The best pairing can be selected based on the value close to 1 in a row vector in the RGA matrix (eq 9). It may be noted that negative values should not be considered for pairing and the sum of all values of a row vector should be equal to 1.

Design of Controller. There are three controllers (i.e., G_{C1}, G_{C2}, and G_{C3}) that must be designed for the best paired manipulated and control variables. The PI settings are computed based on the FOPTD model parameters using the formulas given in Table 1.

Table 1. PI Settings Formulas

methods	K_c	τ_i
IMC[17]	$\frac{\tau}{2K\theta}$	τ
PPM[18,19]	$\frac{1}{K}(4.1045e^{-(1.763(\frac{\theta}{\tau}))})$	$\tau\left(0.311 + 1.372\left(\frac{\theta}{\tau}\right) - 0.545\left(\frac{\theta}{\tau}\right)^2\right)$

Algorithm for Designing Decentralized Controller. The steps involved in the design of a decentralized controller can be summarized as follows:

1. Find the FOPTD models such as (g_{ij}, where i, j = 1, 2, 3).
2. Compute steady-state gain matrix by substituting s = 0 in the estimated FOPTD transfer function model.
3. Find the RGA matrix (Λ) using eq 9.
4. Select the best pairing among the control and manipulated variables. Best pairing can be selected for the pair which has value near to 1 in a RGA row.
5. Design a controller for the best paired transfer function model.

Design of Decoupler. The RGA value indicates the magnitude of the process interactions. A well-known approach to control loop interactions is to design noninteractive control systems. The aim of this controller is to completely eliminate the effects of loop interactions. One of the methods to minimize the interactions is to design a decoupler. The purpose of the decoupler is to break down a multivariate process into several independent single-loop subsystems. The static decoupler can be designed by using the gain value (RGA) of the process at s = 0. Dynamic decoupler works like a lead-lag filter with respect to time. A dynamic decoupler results in better performance than a static decoupler.

From Figure 4, $G_C(s)$, $G_I(s)$, and $G_P(s)$ denote control transfer function matrix, decoupler matrix, and n-dimensional process transfer function matrix, respectively. $G_R(s)$ gives a

DOI: 10.1021/acs.iecr.9b04770
Ind. Eng. Chem. Res. 2019, 58, 20722−20733

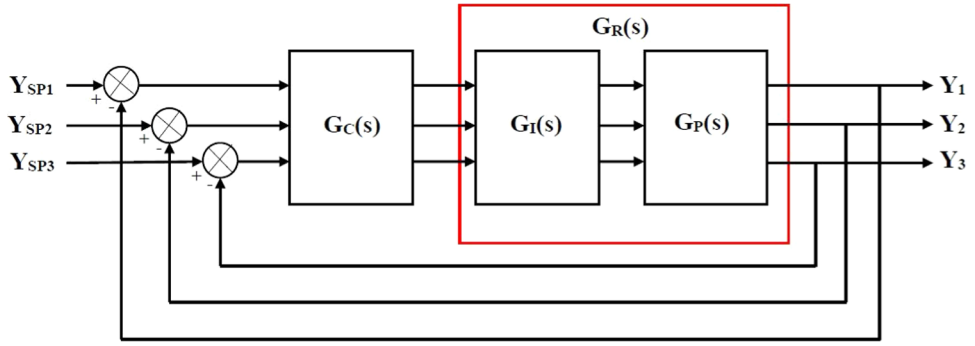

Figure 4. Schematic diagram of decouplers.

proper and casual diagonal matrix for designing the controller of decoupler, and it is given by

$$G_R(s) = G_P(s)G_I(s) \tag{11}$$

where $G_I(s)$ gives a stable and proper decoupler. By multiplying $G_P^{-1}(s)$ on both sides of the above equation, eq 11 can be rewritten as follows

$$G_I(s) = G_P^{-1}(s)G_R(s) \tag{12}$$

The $G_P^{-1}(s)$ value can be computed using dynamic relative gain array (dRGA) as follows

$$\text{dRGA} = \Lambda(s) = G_P(s) \otimes G_P^{-T}(s) \tag{13}$$

$$\Lambda(s) = \begin{pmatrix} g_{11} & g_{12} & g_{13} \\ g_{21} & g_{22} & g_{23} \\ g_{31} & g_{32} & g_{33} \end{pmatrix} \otimes \begin{pmatrix} g_{11} & g_{12} & g_{13} \\ g_{21} & g_{22} & g_{23} \\ g_{31} & g_{32} & g_{33} \end{pmatrix}^{-T} \tag{14}$$

where g_{ij} (where, $i, j = 1, 2, 3$) can be expressed as

$$g_{ij}(s) = \frac{k_{ij}e^{-\theta_{ij}s}}{\tau_{ij}s + 1} \tag{15}$$

$G_P^{-T}(s)$ in eq 13 is called as estimated transfer function array.[20] It is difficult to compute $G_P^{-1}(s)$ for multivariable systems, as one may end up with complicated expressions. According to Shen et al.,[21] $G_P^{-1}(s)$ can be estimated as $G_P^{-1}(s) = \hat{G}_P(s)$. Therefore, eq 14 can be rewritten as

$$\Lambda(s) = G_P(s) \otimes \hat{G}_P^{\,T}(s)$$

$$= \begin{pmatrix} g_{11} & g_{12} & g_{13} \\ g_{21} & g_{22} & g_{23} \\ g_{31} & g_{32} & g_{33} \end{pmatrix} \otimes \begin{pmatrix} \frac{1}{\hat{g}_{11}} & \frac{1}{\hat{g}_{12}} & \frac{1}{\hat{g}_{13}} \\ \frac{1}{\hat{g}_{21}} & \frac{1}{\hat{g}_{22}} & \frac{1}{\hat{g}_{23}} \\ \frac{1}{\hat{g}_{31}} & \frac{1}{\hat{g}_{32}} & \frac{1}{\hat{g}_{33}} \end{pmatrix}^T \tag{16}$$

where $\otimes$ is the hadamard product and $\hat{g}_{ij}$ is given by

$$\hat{g}_{ij} = \frac{k_{ij}/\lambda_{ij}}{\gamma_{ij}\tau_{ij}s + 1}e^{\gamma_{ij}\theta_{ij}s} \tag{17}$$

The parameters involved in eq 17 can be estimated using the RNGA-RGA method, which is discussed in the subsequent sections.

RNGA-RGA Method. The relative normalized gain array (RNGA) is defined as the ratio of normalized gain to the average residence time for loop $i - j$. Average residence time is calculated using $\tau + \theta$, and it represents the response time of a control variable for change in manipulated variables. RNGA can be computed by following

$$\Phi = \text{RNGA} = K_N \otimes K_N^{-T} = \begin{pmatrix} \Phi_{11} & \Phi_{12} & \Phi_{13} \\ \Phi_{21} & \Phi_{22} & \Phi_{23} \\ \Phi_{31} & \Phi_{32} & \Phi_{33} \end{pmatrix} \tag{18}$$

where K_N is the normalized gain array (NGA). It is estimated by following

$$\text{NGA} = K_N = \begin{pmatrix} K_{N,11} & K_{N,12} & K_{N,13} \\ K_{N,21} & K_{N,22} & K_{N,23} \\ K_{N,31} & K_{N,32} & K_{N,33} \end{pmatrix} \tag{19}$$

where $K_{N,ij}$ is the normalized gain and can be expressed as

$$K_{N,ij} = \frac{k_{ij}}{\sigma_{ij}} \tag{20}$$

$\sigma_{ij} = \tau_{ij} + \theta_{ij}$ is the average residence time which gives the response speed of the control variable to manipulated variable.[22] The relative average residence times for all elements of the transfer function matrix can be computed, and the results are entered in an array called the relative average residence time array (RARTA). The RARTA is defined as the ratio of RNGA to RGA values and can be given as follows

$$\Gamma = \text{RARTA} = \begin{pmatrix} \gamma_{11} & \gamma_{12} & \gamma_{13} \\ \gamma_{21} & \gamma_{22} & \gamma_{23} \\ \gamma_{31} & \gamma_{32} & \gamma_{33} \end{pmatrix} \tag{21}$$

The elements of RARTA can be calculated by

$$\gamma_{ij} = \frac{\Phi_{ij}}{\lambda_{ij}} \tag{22}$$

Algorithm for Designing Decoupler. The steps involved in the design of decoupler can be summarized as follows:

1. Calculate the normalized gain ($K_{N,ij}$) using eq 20.
2. Find the normalized gain array (NGA), K_N using eq 19.
3. Using eq 18, compute the relative normalized gain array (RNGA).

DOI: 10.1021/acs.iecr.9b04770
Ind. Eng. Chem. Res. 2019, 58, 20722−20733

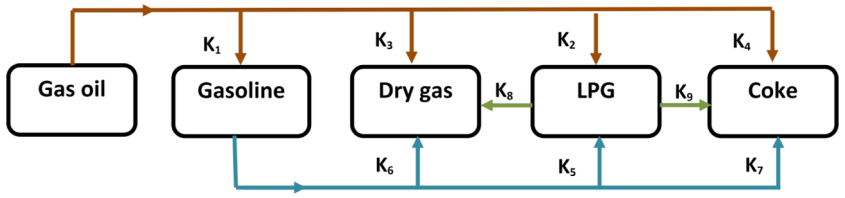

Figure 5. Five-lump parameter model.

4. Determine the relative average residence time array (RARTA) using eq 21, where RARTA matrix elements can be calculated by eq 22.
5. The parameters such as K, NGA, RNGA, and RARTA are substituted in eq 17 to estimate $\hat{G}_P(s)$.
6. The obtained $\hat{G}_P(s)$ and a diagonal matrix $G_R(s)$ are used to compute the decoupler matrix $G_I(s)$.
7. The controllers are designed based on the diagonal elements of $G_R(s)$.

PERFORMANCE EVALUATION

The performances of the decentralized and decoupler systems are evaluated based on the time integral errors. ITAE means integral time weighted absolute error, and is expressed as

$$\text{ITAE} = \int_0^\infty t|e(t)|\mathrm{d}t \tag{23}$$

Integral of absolute error (IAE) is given by

$$\text{IAE} = \int_0^\infty |e(t)|\mathrm{d}t \tag{24}$$

Integral square error (ISE) is given by

$$\text{ISE} = \int_0^\infty e^2(t)\mathrm{d}t \tag{25}$$

Here, $e(t)$ is error input to the controller, which is calculated based on the difference between measured output value from the process and set point value. The smoothness of the controllers is evaluated based on the total variation (TV) in controller outputs and is represented by

$$\text{TV} = \sum_{i=0}^{\infty} |u_{i+1} - u_i| \tag{26}$$

where u_{i+1} and u_i are the values of manipulated variables measured during the control action at different time intervals.

Robust Stability Analysis. The controller is said to be effective when the sensitivity of the control system does not vary a lot due to small changes in the process model. In a multiloop control system, the robustness study becomes essential when the process model includes uncertainties in its parameters.[23] In the case of a process multiplicative input uncertainty ($G(s)[I + \Delta_I(s)]$), the control system can be considered stable if the following condition is satisfied

$$\|\Delta_I(j\omega)\| < \frac{1}{\sigma_I} \tag{27}$$

where σ_I is the maximum singular value of the following closed-loop system $[I + G_c(j\omega)G(j\omega)]^{-1}G_c(j\omega)G(j\omega)$. Similarly, for output multiplicative uncertainty, $G(s)[I + \Delta_o(s)]$, the closed-loop system is stable if it satisfies the following condition

$$\|\Delta_o(j\omega)\| < \frac{1}{\sigma_o} \tag{28}$$

where $\Delta_I(s)$ and $\Delta_o(s)$ are stable, and σ_o is the maximum singular value of the closed-loop system, $[I + G(j\omega)G_c(j\omega)]^{-1}G(j\omega)G_c(j\omega)$. Uncertainties are estimated to be plotted in terms of inverse maximum singular values and frequency. The area under the curve can determine the robustness of the system; the one with more area under the curve is more robust. This method can be used to compare the stability and robustness of the control system.

APPLICATION TO FLUID CATALYTIC CRACKING UNIT

FCCU is one of the important unit operations in petroleum refineries. FCCU gained its importance in the research area due its complexity and economic value of the products it produces. The complexity of the FCCU is mainly due to the high interactions between the control variables and the manipulated variables. In this work, a model is developed including all effects due to interactions in FCCU. Interactions in the process are due to multiple inputs multiple outputs (MIMO). Designing a controller for the system with multiloops is difficult. The decentralized controller method is used to design the controller by breaking the multiple loops

Table 2. Rate Expression

ith reaction	rate of reaction
1,2,3, & 4	$r_i = k_i\phi Y_{go}^2$
5, 6, & 7	$r_i = k_i\phi Y_{ga}$
8 & 9	$r_i = k_i\phi Y_{lpg}$

Table 3. Kinetic Parameters of Five-Lump Parameter Model[25]

i	reaction	frequency factor, k_0	activation energy, E (kJ/kmol)	heat of reaction, H (kJ/kmol)
1	gas oil to gasoline	19 584.55	57 540	45 000
2	gas oil to LPG	3246.215	52 500	159 315
3	gas oil to dry gas	559.9	49 560	159 315
4	gas oil to coke	41.44	31 920	159 315
5	gasoline to LPG	65.40	73 500	42 420
6	gasoline to dry gas	0.00	45 360	42 420
7	gasoline to coke	0.00	66 780	42 420
8	LPG to dry gas	0.32	39 900	2100
9	LPG to coke	0.19	31 500	2100

DOI: 10.1021/acs.iecr.9b04770
Ind. Eng. Chem. Res. 2019, 58, 20722−20733

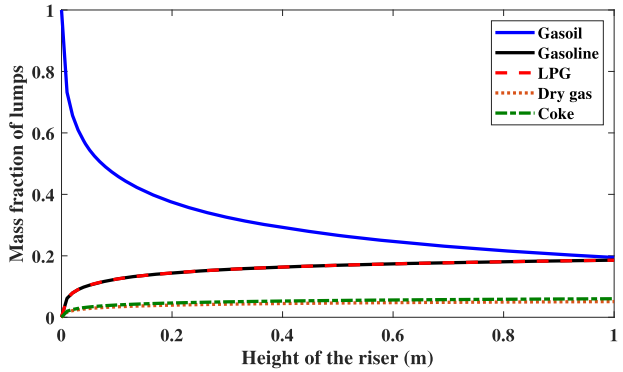

Figure 6. Change in mass fraction of lumps with respect to change in height of the riser reactor.

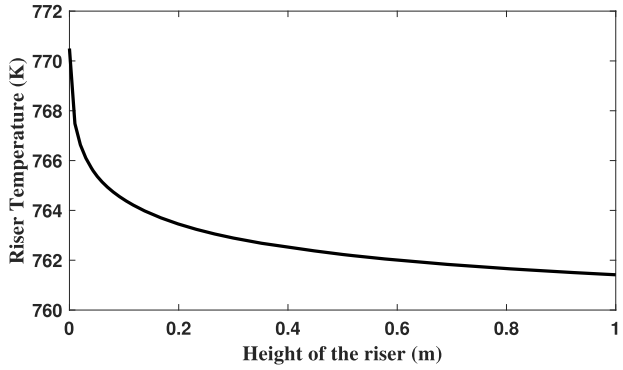

Figure 7. Riser temperature change with respect to change in height of the riser reactor.

Table 4. PI Settings for Decentralized Controller of FCCU

	IMC		PPM	
controllers	K_c	τ_I	K_c	τ_I
G_{C1}	0.3408	41.1782	0.4070	23.7331
G_{C2}	24.716	41.4730	7.2659	15.045
G_{C3}	8.8548	44.55	2.6260	16.1827

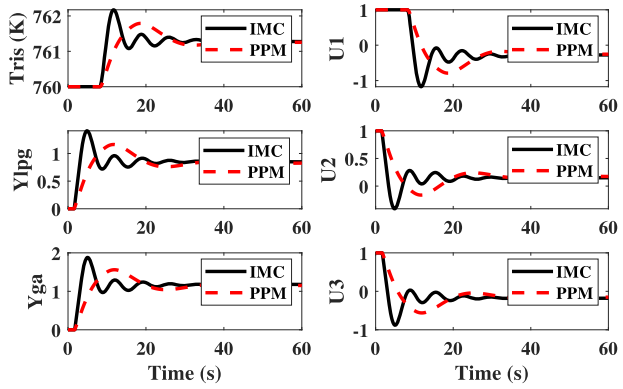

Figure 8. Closed-loop servo response and change in manipulated variables for decentralized FCCU.

into n^2 single loops. Even though controllers are designed, sometimes due to high interactions, they may affect the stability of the process. To reduce the interactions, it is necessary to design the decouplers for the process.

Mathematical Model of Riser. Gas oil is converted to gasoline and LPG only in the riser reactor. Gasoline and LPG have more economic importance compared to other products in the riser reactor. Due to this reason, the riser reactor is considered for modeling.

A lumping strategy is used for the characterization of the cracking reactions. In the lump model, the feed cracks into some lumps like gas oil, gasoline, LPG, dry gas, coke, etc. as products of these reactions. A five-lump model strategy is considered in this study. Gas oil, gasoline, LPG, dry gas, and coke are assumed as five lumps in the model. Because of their economic importance, gasoline and LPG are considered in the five lumps. Dry gas and coke are recommended because of their effect on the performance of the riser. A schematic representation of the five-lump model is shown in Figure 5. There are nine different reactions taking place in the five-lump parameter model. The mass fractions of gas oil, gasoline, LPG, dry gas, and coke are represented as Y_{go}, Y_{ga}, Y_{lpg}, Y_{dg}, and Y_c, respectively.[24] The mathematical models for mass fractions are developed based on the first-principles approach. Eqs 29−33 represent the differential equations for mass fractions with respect to the height of the riser. The variation of the temperature (T_{ris}) along the length of the riser can be obtained from the energy balance equation

$$\frac{dY_{go}}{dz} = -\frac{A_{ris}H_{ris}\phi(1-\epsilon)\rho_c}{F_{feed}}(k_1 + k_2 + k_3 + k_4)Y_{go}^2 \tag{29}$$

$$\frac{dY_{ga}}{dz} = \frac{A_{ris}H_{ris}\phi(1-\epsilon)\rho_c}{F_{feed}}(k_2Y_{go}^2 - k_5Y_{ga} - k_6Y_{ga} - k_7Y_{ga}) \tag{30}$$

$$\frac{dY_{lpg}}{dz} = \frac{A_{ris}H_{ris}\phi(1-\epsilon)\rho_c}{F_{feed}}(k_3Y_{go}^2 + k_6Y_{ga} + k_8Y_{lpg}) \tag{31}$$

$$\frac{dY_{dg}}{dz} = \frac{A_{ris}H_{ris}\phi(1-\epsilon)\rho_c}{F_{feed}}(k_3Y_{go}^2 + k_5Y_{ga} - k_8Y_{lpg} - k_9Y_{lpg}) \tag{32}$$

$$\frac{dY_c}{dz} = \frac{A_{ris}H_{ris}\phi(1-\epsilon)\rho_c}{F_{feed}}(k_4Y_{go}^2 + k_7Y_{ga} + k_9Y_{lpg}) \tag{33}$$

$$\frac{dT_{ris}}{dz} = -\frac{A_{ris}H_{ris}\phi(1-\epsilon)\rho_c}{F_{feed}T_m((F_{rgc}C_{pc}) + (F_{feed}C_{pfv}))}\sum_{i=1}^{9}(r_i\Delta H_i) \tag{34}$$

Due to several factors, catalyst deactivation can take place in the FCC process. Because of attrition and high temperatures, catalyst pellets may lose their mass. The deactivation of the catalyst must be considered during the modeling because of its importance in determining the life cycle of catalyst. The catalyst activity can be expressed as follows

$$\phi = (1 + 51Y_c)^{-2.78} \tag{35}$$

The void fraction of the catalyst bed in the riser is given as

$$\epsilon = \frac{\frac{F_{feed}}{\rho_v}}{\frac{F_{feed}}{\rho_v} + \frac{F_{rgc}}{\rho_c}} \tag{36}$$

Gas oil enters the riser in the form of vapor. Since the density of the vapor varies with the riser temperature, it can be determined by the following expression

DOI: 10.1021/acs.iecr.9b04770
Ind. Eng. Chem. Res. 2019, 58, 20722−20733

Table 5. Closed-Loop Servo Performance Indices in Terms of Errors and TV

	IMC				PPM			
	ITAE	IAE	ISE	TV	ITAE	IAE	ISE	TV
T_{ris}	75.4	4.1	0.51	0.24	59.9	3.2	0.31	0.19
Y_{ga}	3533	147.2	564.7	6.47	2099	77.43	143.6	0.63
Y_{lpg}	1202	53.54	83.57	4.73	491.4	20.71	10.84	1.6

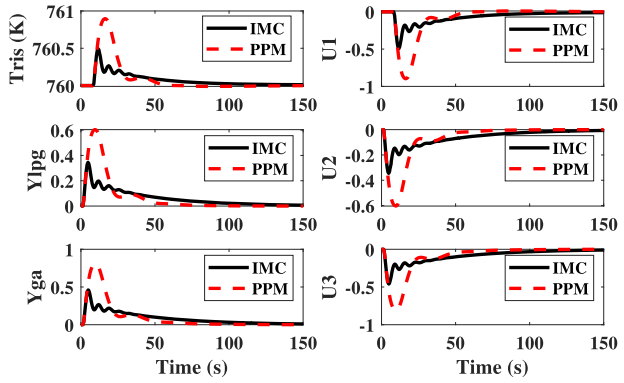

Figure 9. Closed-loop regulatory performance and change in manipulated variables for decentralized FCCU.

$$\rho_v = \frac{P_{ris} MW_{gasoil}}{RT_{ris}} \tag{37}$$

Gas oil vapor feed and regenerated catalyst flow will be mixed at the entry of riser. A significant change of temperature takes place due to the mixing operation. To quantify the temperature of the mixture (T_m) at $z = 0$, the following expression can be used

$$T_m = \frac{F_{rgc}C_{pc}(T_{rgn} - 10) + (F_{feed}C_{pfl}T_f) - \Delta H_{evp}F_{feed} - Q_{loss,ris}}{(F_{rgc}C_{pc}) + (F_{feed}C_{pfv})} \tag{38}$$

The heat losses during the mixing are taken into consideration and can be computed as follows

$$Q_{loss,ris} = 0.019(F_{rgc}C_{pc}(T_{rgn} - 10) + (F_{feed}C_{pfl}T_f) - (\Delta H_{evp}F_{feed})) \tag{39}$$

Rate equations for the nine reactions shown in Figure 5 are divided into three categories based on the common reactant. The first category concerns the gas oil products. There are four gas oil products, gasoline, LPG, dry gas, and coke. Similarly, the second and third categories are based on the products formed from gasoline and LPG, respectively. The modeling does not take into account the reversible reactions and conversion of dry gas to coke.[24] The rate expression for the ith reaction is given in Table 2.

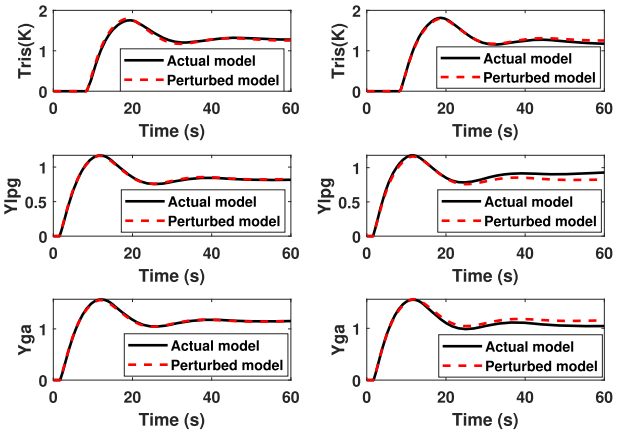

Figure 10. Robustness comparison +10% perturbation in process delay (left column); +10 % perturbation in process gain (right column).

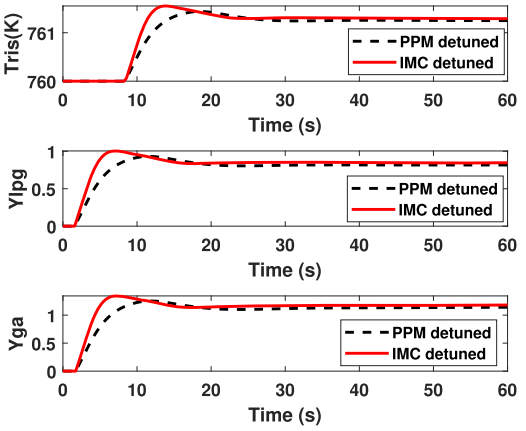

Figure 11. Performance of detuned controller.

The rate constant for ith reaction is given by the Arrhenius equation as follows

$$k_i = k_{0,i}e^{(-E_i/RT_{ris})}$$

Frequency factor units for i = 1, 2, 3, and 4 are $m^6/$(kg catalyst)(kmol gas oil)(S) and for remaining reactions, $m^3/$(kg catalyst)(S) which are given in Table 3. The model equations are solved using MATLAB, and the change in state variables with respect to height of the riser is obtained. The obtained

Table 6. Closed-Loop Regulatory Performance Indices in Terms of Errors and TV

	IMC				PPM			
	ITAE	IAE	ISE	TV	ITAE	IAE	ISE	TV
T_{ris}	7214	58.05	14.44	0.24	2964	22.84	2.183	0.1
Y_{ga}	175 000	1392	7839	5.59	155 000	1230	6138	4.94
Y_{lpg}	81 900	654.2	1734	2.59	73 600	581.6	1374	2.34

DOI: 10.1021/acs.iecr.9b04770
Ind. Eng. Chem. Res. 2019, 58, 20722−20733

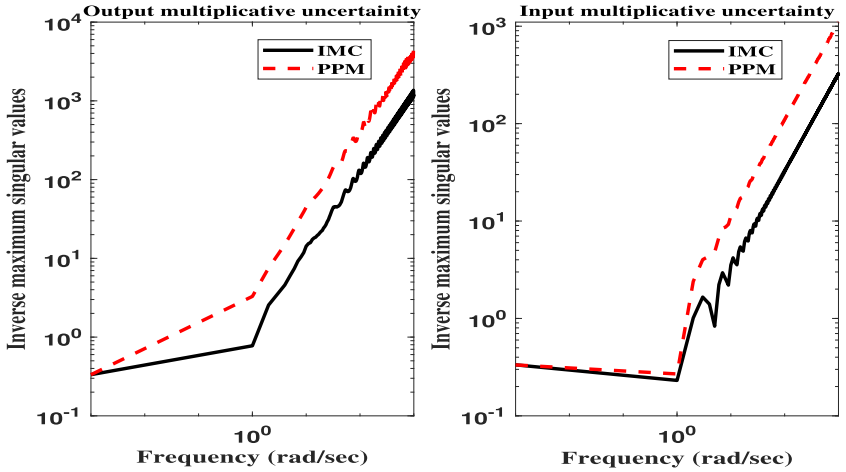

Figure 12. Stability region of output and input uncertainties of decentralized FCCU. Left: output uncertainties; right: input uncertainties.

Table 7. PI Settings Used in the Decoupler

	IMC		PPM	
controllers	K_c	τ_I	K_c	τ_I
G_{C1}	2.3397	5.545	2.8160	3.2123
G_{C2}	13.0497	55.558	3.8364	20.1547
G_{C3}	12.9274	129.6	3.8339	47.0772

results are shown in Figures 6 and 7. Figure 6 represents the change in mass fractions along the height of the riser. Similarly, Figure 7 shows the change of riser temperature for a change in height of the riser.

Identification of FCC Unit. In this study, T_{ris}, Y_{lpg}, and Y_{ga} are considered to be the control variables because they are key process variables in FCCU. The regenerated feed rate (F_{rgc}), the feed temperature (T_f), and the regenerated catalyst temperature (T_{rgn}) are chosen as manipulated variables for the control of T_{ris}, Y_{lpg}, and Y_{ga}. The elements of $G_P(s)$ matrix are estimated using the process reaction curve method and is given in the following equation

$$G_P(s) = \begin{pmatrix} \frac{6.95e^{-8.698s}}{41.178s+1} & \frac{0.812e^{-8.551s}}{40.896s+1} & \frac{1.57e^{-8.254s}}{40.327s+1} \\ \frac{4.51e^{-1.589s}}{41.473s+1} & \frac{0.528e^{-1.589s}}{41.473s+1} & \frac{1.02e^{-1.589s}}{41.473s+1} \\ \frac{6.44e^{-1.723s}}{44.55s+1} & \frac{0.753e^{-1.723s}}{44.55s+1} & \frac{1.46e^{-1.723s}}{44.55s+1} \end{pmatrix} \quad (40)$$

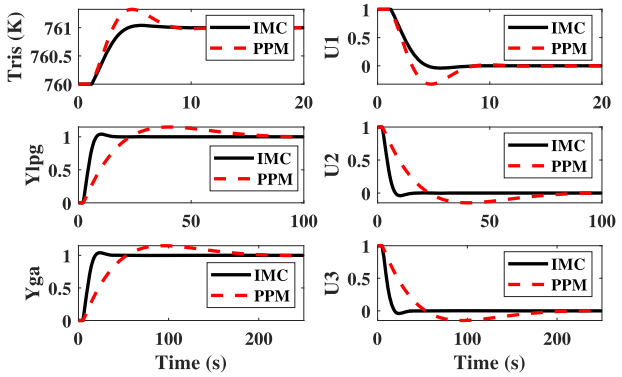

Figure 14. Closed-loop performance and change in manipulated variables for decentralized FCCU with decouplers.

Design of Decentralized Controller. The gain array matrix can be estimated by substituting $s = 0$ in eq 40

$$\text{gain matrix} = K = \begin{pmatrix} 6.95 & 0.812 & 1.57 \\ 4.51 & 0.528 & 1.02 \\ 6.44 & 0.753 & 1.46 \end{pmatrix} \quad (41)$$

The RGA can be calculated using eq 9 as

$$\text{RGA} = \Lambda = \begin{pmatrix} 574.75 & -376.23 & -197.52 \\ -437.77 & 560.52 & -121.74 \\ -135.98 & -183.28 & 320.26 \end{pmatrix} \quad (42)$$

Based on the RGA values calculated above, the best pairing for the values in a row that are closer to 1 and non-negative can be

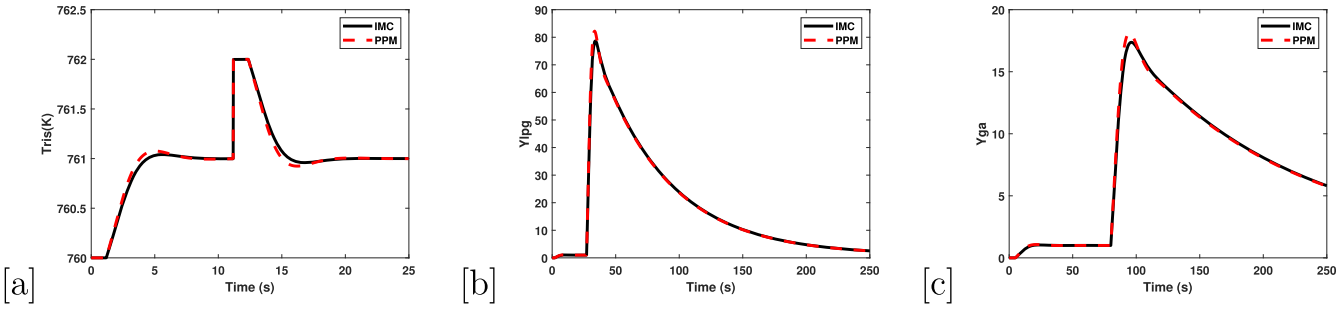

Figure 13. Closed-loop performance due to change in load variables (a) T_{ris}, (b) Y_{lpg}, and (c) Y_{ga}.

DOI: 10.1021/acs.iecr.9b04770
Ind. Eng. Chem. Res. 2019, 58, 20722−20733

Table 8. Closed-Loop Performance Indices for Decentralized FCCU with Decouplers in Terms of Errors and TV

	IMC				PPM			
	ITAE	IAE	ISE	TV	ITAE	IAE	ISE	TV
T_{ris}	4.04	2.57	1.99	1.82	8.22	3.16	2.05	1.34
Y_{ga}	5.22	1.85	0.57	4.82	137.9	6.39	1.25	1.13
Y_{lpg}	28.92	4.35	1.35	4.77	730.4	14.85	2.93	1.14

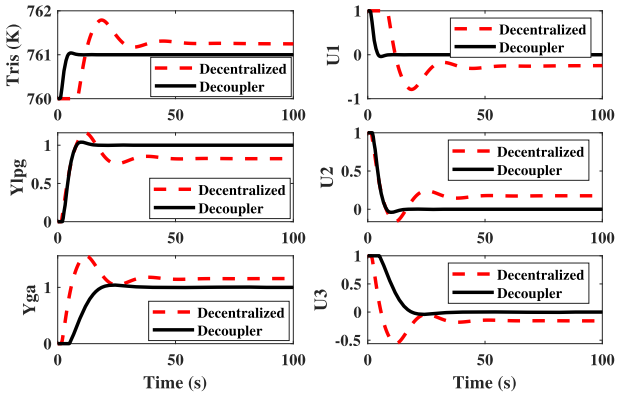

Figure 15. Closed-loop performance comparison of decentralized controller and system with decouplers.

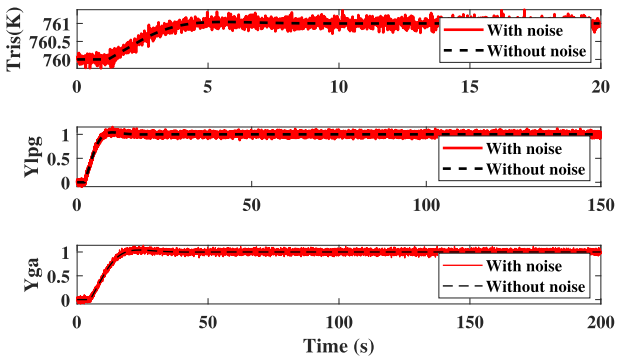

Figure 16. Closed-loop servo response with and without noise for the decoupler control system.

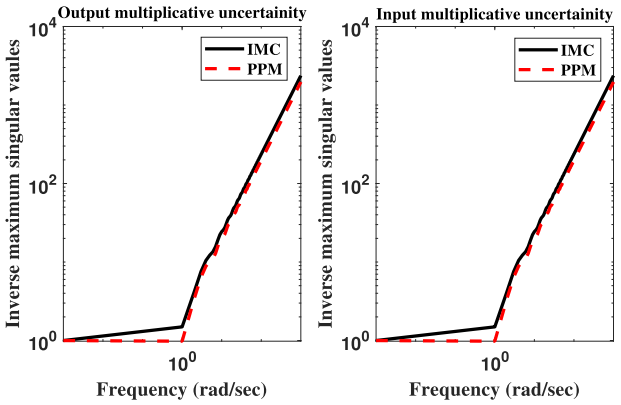

Figure 17. Output and input multiplicative uncertainty of decentralized FCCU with decoupler.

identified. It is clear from eq 42 that the best pairing can be given for the following $T_{ris}-F_{rgc}$, $Y_{lpg}-T_f$, and $Y_{ga}-T_{rgn}$. For the present work, the PI controllers are designed for the best paired control and manipulated variable using IMC and PPM methods. The estimated PI settings for the decentralized controller are enlisted in Table 4.

The designed set of PI settings is implemented on the decentralized FCCU, and the closed-loop performances are obtained. The closed-loop performances of control variables (T_{ris}, Y_{LPG}, and Y_{Ga}) are evaluated by introducing a step input to the steady-state temperature of the riser, and the resulted responses are shown in Figure 8. In Figure 8, the closed-loop servo responses are shown on the left-hand side, and the variation of manipulated variables is shown on the right-hand side. From Figure 8, it can be seen that both the controllers could stabilize the process at the same settling time. The response obtained from the PPM method, however, results in lower overshoot and rise time compared to the IMC method. Quantitative analysis is also carried out in terms of time integral errors such as ITAE, IAE, and ISE, and the results are given in Table 5. It is clear from Table 5 that PPM has lowest error indices in all three controllers. The ISE for the PPM method is reduced from 0.51 to 0.31 for the riser temperature, a reduction of 40%, compared to the IMC method. Similarly, for Y_{LPG} and Y_{Ga} responses, there is a 75 and 87% reduction in ISE index for the PPM method, respectively. The TV value gives the variation in the manipulated variables for maintaining the control variables in steady state. Smooth performance of manipulated variable can be achieved for controllers with lower TV values. Table 5 shows that the PPM method has lower TV values compared to IMC.

In industries, the common control problems arise due to the disturbance in input to the process. In the present work, the performance of the two methods for the regulatory problem is evaluated by introducing a step input into the load variable, and the resulted responses are shown in Figure 9 (left-hand side). The variation of the manipulated variable for the regulator problem is also estimated for the two methods and is shown in Figure 9 (right-hand side). An improved closed-loop performance is achieved by the PPM method.

From Figure 9, both the methods have been shown to stabilize the responses. However, the PPM method has a shorter settling time and lesser oscillations compared to the IMC method. Table 6 shows that the PPM tuning method shows better control performance compared to the IMC method by reducing the ISE value by approximately 85, 22, and 21%, respectively, for T_{ris}, Y_{LPG}, and Y_{Ga} responses. Based on the TV values in Table 6, it is clear that the PPM tuning method gives smoother control performance than IMC. The closed-loop performance of the decentralized controller for perturbation in each time delay and process gain is evaluated, and the servo responses for a unit step change in the set point are given in Figure 10. From the rigorous simulation studies, it is found that the decrease in process gain results in an unstable response. However, the control system produces a stable closed-loop response for the positive increment in the process gain (i.e., +1, +5, +10%, etc.), as shown in Figure 10.

Due to the presence of interactions in multiloop control system, design of controller for such systems is cumbersome.

DOI: 10.1021/acs.iecr.9b04770
Ind. Eng. Chem. Res. 2019, 58, 20722−20733

The idea here is to design controller settings for multiloop system by adopting single-input single-output design approaches. The designed controllers are then detuned to negate the effects of the interactions. The detuning is done to get an appropriate trade-off between the stability and the closed-loop performance. The goal of detuning is to achieve a suitable trade-off between performance and relative stability. A method proposed by Luyben[26] is given as follows

$$\hat{k}_c = \frac{k_c}{F};\ \ \hat{\tau}_I = \tau_I F \tag{43}$$

where $\hat{k}_c$ and $\hat{\tau}_I$ are detuned controller gain and integral time constant, respectively, and F is the detuning factor.[27] The optimum value of F can be determined by minimizing the integral of square error for the set point tracking problem using MATLAB *fminsearch* solver aimed at providing supreme stability. The detuning of decentralized PI controller settings for an FCCU has been carried out using an optimization-based approach. The optimum detuning parameter (F) is found to be 1.852. The closed-loop responses obtained based on the optimum detuning parameter are shown in Figure 11. From Figure 11, it can be seen that the controller achieves stability. However, the PPM method shows superior response to the IMC method.

The robustness study is also carried out based on uncertainties in the multiple inputs and the outputs. The uncertainties in the process are computed by finding the inverse maximum singular values of the closed-loop decentralized FCCU. As stated earlier, the stability limits of the closed-loop system can be obtained from eqs 27 and 28. Figure 12 gives the stability bounds of the closed-loop responses obtained from the two methods. It is to be noted that the region below the curve denotes the stability region, whereas the region of instability is above the curve. A controller is also said to be more robust if the area below the curve is large. From Figure 12, it can be observed that the controller designed by the PPM method has a greater stability region than the controller obtained from the IMC method, which means that the former has more robust stability.

Design of Decoupler. As discussed earlier, the decoupler design starts with the computation of the normalized gain array (NGA). According to eq 19, NGA is given by

$$\text{NGA} = K_N = \begin{pmatrix} -76.98 & 50.83 & 27.16 \\ -317.6 & 481.69 & -163.09 \\ 395.58 & -531.51 & 136.93 \end{pmatrix} \tag{44}$$

RNGA can be calculated by substituting NGA into eq 18

$$\text{RNGA} = \Phi = \begin{pmatrix} -76.98 & 50.83 & 27.16 \\ -317.6 & 481.69 & -163.09 \\ 395.58 & -531.51 & 136.93 \end{pmatrix} \tag{45}$$

By using the preceding concepts, the elements of the RARTA matrix are calculated by eq 22 as

$$\text{RARTA} = \Gamma = \begin{pmatrix} 0.134 & 0.135 & 0.136 \\ 0.725 & 0.859 & 1.34 \\ 2.91 & 2.9 & 0.428 \end{pmatrix} \tag{46}$$

The elements of the estimated transfer function matrix (refer eq 17) are found as

$$\hat{G_P}^T(s) = \begin{pmatrix} \frac{5.515s+1}{0.0121}e^{1.16s} & \frac{30.088s+1}{-0.0108}e^{1.153s} & \frac{129.6s+1}{-0.047}e^{5.0126s} \\ \frac{5.525s+1}{-0.00216}e^{1.155s} & \frac{35.64s+1}{0.001}e^{1.365s} & \frac{129.19s+1}{-0.0041}e^{4.99s} \\ \frac{5.545s+1}{-0.0079}e^{1.185s} & \frac{55.56s+1}{-0.0084}e^{2.129s} & \frac{19.048s+1}{0.0045}e^{0.786s} \end{pmatrix} \tag{47}$$

The diagonal matrix $G_R(s)$ is given by

$$G_R(s) = \begin{pmatrix} \frac{e^{-1.185s}}{5.545s+1} & 0 & 0 \\ 0 & \frac{e^{-2.129s}}{55.56s+1} & 0 \\ 0 & 0 & \frac{e^{-5.0126s}}{129.6s+1} \end{pmatrix} \tag{48}$$

The decoupler is estimated as

$$G_I(s) = \begin{pmatrix} \frac{82.713(5.155s+1)}{(5.545s+1)}e^{-0.0206s} & \frac{-92.59(30.088s+1)}{(55.56s+1)}e^{-0.9759s} & -21.115 \\ \frac{-463.39(5.5247s+1)}{(5.545s+1)}e^{-0.03s} & \frac{1063.83(35.64s+1)}{(55.56s+1)}e^{-0.7632s} & \frac{-243.9(129.19s+1)}{(129.6s+1)}e^{-0.0226s} \\ -125.786 & -119.048 & \frac{222.22(19.048s+1)}{129.6s+1}e^{-4.226s} \end{pmatrix} \tag{49}$$

The PI controller settings can be designed for the diagonal elements of $G_R(s)$. The same methods used for the design of the decentralized controller are used here for the design of the decoupler control system. The PI settings are determined using the IMC and PPM methods and are given in Table 7 (Figure 13).

The closed-loop performance can be evaluated on the basis of parameters such as rise time, oscillation, and settling time. The closed-loop response of the decentralized FCCU with decoupler is evaluated by introducing step input to the steady-state temperature of the riser. Figure 14 shows the comparison of the closed-loop servo responses obtained from the IMC and PPM methods for the decoupler control system. The variation of the manipulated variable is also shown in Figure 14. The quantitative analysis of the closed-loop performances is carried out, and the results are presented in Table 8. It is evident from Table 8 that the IMC shows enhancement in controller performance compared to the PPM tuning method by reduction of ISE with 51, 97, and 96% for T_{ris}, Y_{LPG}, and Y_{Ga}, respectively. The TV values in Table 8 show that the PPM

DOI: 10.1021/acs.iecr.9b04770
Ind. Eng. Chem. Res. 2019, 58, 20722−20733

provides improved controller performance. However, the PPM method reports very large errors compared to the IMC method. It can be seen from the decoupler matrix that the models have larger gains. It is well known that the decoupler with large gains is quantifiably more difficult to control when there is a disturbance in the process. Simulation studies have been performed to show that the larger-gain decoupler takes more time to stabilize when there is a change in the load variable. The closed performance is evaluated for a unit step change in the load variable at t = 10, 25, and 75 s for T_{ris}, Y_{lpg}, and Y_{ga}, respectively. The obtained responses are shown in Figure 13.

A comparison of closed-loop performance of the decentralized controller and the system with decouplers is given in Figure 15. Clearly, the closed-loop response of the decentralized controller has more oscillations, rise time, and settling time. This can be caused due to high interaction between the multiloops. The decouplers can reduce the interaction between the multiloops. Compared to the decentralized controller, the decoupler produces superior response in terms of overshoot, number of oscillations, rise time, and settling time, as shown in Figure 15. For the decoupler controller, the effect of measurement noise on the closed-loop response has been assessed by introducing random noise of variances 1, 0.1, and 0.1, respectively, to the measurement value of T_{ris}, Y_{lpg}, and Y_{ga}. The closed servo response of the FCCU with decoupler under the same PI settings with and without measurement noise is shown in Figure 16. The simulation results show a good closed-loop servo response even in the presence of measurement noise. The robustness plot for the decoupler is shown in Figure 17, and from the figure, it may be inferred that the IMC controllers have a larger stability region, which signifies that the IMC method is more robust.

CONCLUSIONS

This paper presents a decoupling control system for an FCCU to account for the high interaction among multiloops. Based on the FOPTD model of the five-lump kinetic model of FCCU, a decentralized PI controller has been designed and implemented on the FCCU unit and the closed-loop servo and regulatory responses have been obtained. The robustness studies show that the PPM method is found to be more robust. To reduce the interactions among the multiloops, a decoupler is designed by the RNGA and dRGA methods and evaluated on the FCCU. It is observed that the decoupler gives good dynamic closed-loop performance for a set point tracking and disturbance rejection problems.

AUTHOR INFORMATION

Corresponding Author

*E-mail: csrao@nitk.edu.in. Phone: 0824 247 3639. Fax: 0824 247 4033.

ORCID

C. Sankar Rao: 0000-0002-3554-5006

Notes

The authors declare no competing financial interest.

NOMENCLATURE

ΔH_i	heat of ith reaction, kJ/kg
ϵ	void fraction of riser
ϕ	catalyst activity
ρ_c	catalyst density, kg/m^3
ρ_v	vapor density of gas oil, kg/m^3
A_{rgn}	cross-sectional area of the regenerator, m^2
A_{ris}	cross-sectional area of the riser, m^2
C_{pc}	catalyst specific heat, kJ/(kg K)
C_{pfl}	specific heat capacity of liquid feed, kJ/(kg K)
C_{pfv}	specific heat capacity of vapor feed, kJ/(kg K)
E_i	activation energy of ith reaction, kJ/kmol
F_{feed}	gas oil feed rate, kg/s
F_{rgc}	regenerated catalyst flow rate, kg/s
H_{evp}	heat of vaporization of gas oil feed, kJ/kg
H_{ris}	geight of the riser, m
K_i	rate constant of ith reaction
K_{oi}	frequency factor of ith reaction
MW_{coke}	molecular weight of coke, kg/kmol
$MW_{dry\ gas}$	molecular weight of dry gas, kg/kmol
$MW_{gas\ oil}$	molecular weight of gas oil, kg/kmol
$MW_{gasoline}$	molecular weight of gasoline, kg/kmol
MW_{LPG}	molecular weight of LPG, kg/kmol
P_{ris}	riser pressure, atm
$Q_{loss,ris}$	heat losses from the riser, kJ/s
R	universal gas constant, J/(mol K)
r_i	rate of ith reaction
T_f	feed gas oil temperature, K
T_m	mean temperature at any axial height of riser, K
T_{rgn}	temperature of the regenerator, K
T_{ris}	riser temperature, K
Y_c	mass fraction of coke
Y_{dg}	mass fraction of dry gas
Y_{ga}	mass fraction of gasoline
Y_{go}	mass fraction of gas oil
Y_{lpg}	mass fraction of LPG
Z	height of the riser, m

REFERENCES

(1) Ali, H.; Rohani, S.; Corriou, J. Modelling and Control of a Riser Type Fluid Catalytic Cracking (FCC) Unit. *Chem. Eng. Res. Des.* **1997**, *75*, 401−412.

(2) John, Y.; Mustafa, M.; Patel, R.; Mujtaba, I. Parameter estimation of a six-lump kinetic model of an industrial fluid catalytic cracking unit. *Fuel* **2019**, *235*, 1436−1454.

(3) Malay, P.; Rohani, S.; Milne, B. J. The modified dynamic model of a riser type fluid catalytic cracking unit. *Can. J. Chem. Eng.* **1999**, *77*, 169−179.

(4) Shayegh, F.; Farshi, A.; Dehgan, A. A Kinetics Lumped Model for VGO Catalytic Cracking in a Fluidized Bed Reactor. *Pet. Sci. Technol.* **2012**, *30*, No. 945957.

(5) Sadeghzadeh Ahari, J.; Farshi, A.; Forsat, K. A mathematical modeling of the riser reactor in industrial FCC unit. *Pet. Coal* **2008**, *50*, 15−24.

(6) Arbel, A.; Huang, Z.; Rinard, I. H.; Shinnar, R.; Sapre, A. V. Dynamic and Control of Fluidized Catalytic Crackers. 1. Modeling of the Current Generation of FCC's. *Ind. Eng. Chem. Res.* **1995**, *34*, 1228−1243.

(7) Dagde, K.; Puyate, Y. T. Modelling and Simulation of Industrial FCC Unit: Analysis based on Five-Lump kinetic scheme for gas-oil cracking. *Int. J. Eng. Res. Ind. Appl.* **2012**, *2*, 698−714.

(8) Ansari, R.; Tad, M. Constrained nonlinear multivariable control of a fluid catalytic cracking process. *J. Process Control* **2000**, *10*, 539−555.

(9) Jarullah, A.; Awad, N.; Mujtaba, I. Optimal design and operation of an industrial fluidized catalytic cracking reactor. *Fuel* **2017**, *206*, 657−674.

DOI: 10.1021/acs.iecr.9b04770
Ind. Eng. Chem. Res. 2019, 58, 20722−20733

(10) Alvarez-Ramirez, J.; Monroy-Loperena, R. A PI control configuration for a class of MIMO processes. *Ind. Eng. Chem. Res.* **2001**, *40*, 1186−1199.
(11) Devikumari, A.; Vijayan, V. Decentralised PID controller design for 3 × 3 multivariable systems using heuristic algorithms. *Indian J. Sci. Technol.* **2015**, *8*, 1−6..
(12) Rajapandiyan, C.; Chidambaram, M. Controller Design for MIMO Processes Based on Simple Decoupled Equivalent Transfer Functions and Simplified Decoupler. *Ind. Eng. Chem. Res.* **2012**, *51*, 12398−12410.
(13) Sundaresan, K. R.; Krishnaswamy, P. R. Estimation of time delay time constant parameters in time, frequency, and laplace domains. *Can. J. Chem. Eng.* **1978**, *56*, 257−262.
(14) Chidambaram, M.; Rao, C. S. *Subspace Identification of Dynamic Systems*, 1st ed.; Narosa Publisher: New Delhi, 2017.
(15) Stephanopoulos, G. *Chemical Process Control: An Introduction to Theory and Practice*, 18th ed.; Prentice-Hall, 1984.
(16) Seborg, D. E.; Edgar, T. F.; Mellichamp, D. A. *Dynamics and Control*, 2nd ed.; Wiley, 2004.
(17) Skogestad, S. Simple Analytic Rules for Model Reduction and PID Controller Tuning. *J. Process Control* **2004**, *13*, 291−309.
(18) Padma Sree, R.; Srinivas, M.; Chidambaram, M. A simple method of tuning PID controllers for stable and unstable FOPTD systems. *Comput. Chem. Eng.* **2004**, *28*, 2201−2218.
(19) Sankar Rao, C.; Chidambaram, M. Subspace Identification of Transfer Function Models for an Unstable Bioreactor. *Chem. Eng. Commun.* **2015**, *202*, 1296−1303.
(20) Vijay Kumar, V.; Rao, V. S.; Manickam, C. Centralized PI controllers for interacting multivariable processes by synthesis method. *ISA Trans.* **2012**, *51*, 400−409.
(21) Shen, Y.; Cai, W.-J.; Li, S. Normalized decoupling control for high-dimensional MIMO processes for application in room temperature control HVAC systems. *Control Eng. Pract.* **2010**, *18*, 652−664.
(22) He, M.-J.; Cai, W.-J.; Ni, W.; Xie, L.-H. RNGA based control system configuration for multivariable processes. *J. Process Control* **2009**, *19*, 1036−1042.
(23) Besta, C. S.; Chidambaram, M. Improved Decentralized Controllers for Stable Systems by IMC Method. *Indian Chem. Eng.* **2018**, *60*, 418−437.
(24) Dave, D.; Saraf, D. Model for rating and optimization of industrial FCC units. *Indian Chem. Eng.* **2003**, *45*, 7−19.
(25) Sinha, S.; Praveen, C. Optimization of Industrial Fluid Catalytic Cracking Unit having Five Lump Kinetic Scheme using Genetic Algorithm. *Comput. Model. Eng. Sci.* **2008**, *32*, 85−101.
(26) Luyben, W. L. Simple method for tuning SISO controllers in multivariable systems. *Ind. Eng. Chem. Process Des. Dev.* **1986**, *25*, 654−660.
(27) Khandelwal, S.; Detroja, K. P. *Optimal Detuning Parameter Design for Decentralized Control of MIMO Processes*, TENCON 2017—2017 IEEE Region 10 Conference, 2017; pp 597−601.

DOI: 10.1021/acs.iecr.9b04770
Ind. Eng. Chem. Res. 2019, 58, 20722−20733